Nigerian Research Journal of Engineering and Environmental Sciences 4(2) 2019 pp. 746-755

Nigerian Research Journal of Engineering and Environmental Sciences
Journal homepage: www.rjees.com

Original Research Article

Power Quality Enhancement for a Standalone Photovoltaic System

[1]Oluseyi, P.O., [1]Akinbulire, T.O., [1]Ugherughe, J., [2]Oladoyinbo, O. and *[1]Babatunde, O.M.

[1]Department of Electrical and Electronics Engineering, University of Lagos, Akoka, Yaba, Lagos, Nigeria.
[2]Centre for Radio Access, Rural Technologies (COE), University of KwaZulu-Natal, Durban, South Africa.
*mobabatunde@unilag.edu.ng; poluseyi@unilag.edu.ng

ARTICLE INFORMATION

Article history:
Received 04 Jul, 2019
Revised 04 Dec, 2019
Accepted 06 Dec, 2019
Available online 30 Dec, 2019

Keywords:
Power factor compensator
Power quality
Power distribution
Photovoltaic system
Voltage stability

ABSTRACT

A distribution network connected to rural consumers is often quite weak due to the long distance. Hence, an increase in power demand over this network will result to power quality problems. The main cause of this unacceptable situation is the inability of the power system to meet the demand of reactive power. Inductive loads are the main cause of power quality problems and they are widely used in domestic and industrial sector, contributing to inefficient use of energy. In this paper, a reactive power compensator is proposed to give voltage stabilization, good power quality and to control non-linear loads in a standalone photovoltaic system. The results obtained show significant enhancement in terms of power factor correction of 0.87, thereby improving the power quality of the system.

1. INTRODUCTION

As power generating plants are typically situated far away from the city, significant loss is experienced in the course of operating the transmission lines (Bayliss, 2012). Similarly, commercial grid system fluctuations are dependent on peak periods of power load demand, which sometimes result to insufficiency of the grid as the maximum output power margin of the grid is exceeded (Gonen, 2014). In addition, interconnected grids tend to become more unstable as loads vary dynamically in magnitude, phase and power factor (Rohouma *et al.,* 2019). This voltage instability is more noticeable when there is a decrease in magnitude of load.

For example, the distribution network connected to rural consumers is often quite weak due to the distance, as they are far away from the generator. Therefore, an increase in power demand over this network will result to power quality problem such as voltage imbalance, high total harmonic distortion and low power factor (Rohouma *et al.,* 2019). The main cause of this unacceptable situation is the inability of the power system to meet the demand of reactive power quantity for sustaining the healthy operation of the system (Madhusudan and Rao, 2012; Masoud and Hussain, 2013).

Ideally, the voltage magnitude of the load bus increases as reactive power injected to the same bus is increased. If the voltage magnitude of a particular bus decreases with an increase in the corresponding reactive power flow, the system is said to be unstable .i.e. the receiving end (node) voltage at the output of the bus is unstable (Amroune et al., 2014).

Further to this, the major factors causing voltage instability are due to disturbance, which can either be an increase in load or voltage drop, that occurs when active and reactive power flow through the inductive reactance resulting to a gradual and uncontrollable decrease in voltage magnitude. Most importantly, the inability of the system to meet the reactive power requirement, i.e. a mismatch between supply and demand of reactive power, will also result in voltage instability. The voltage decreases slowly as the demand increases until a critical point is reached (Samuel et al., 2012). Although, the voltage instability is a localized problem, its impact on the system depends on the relationship between transmitted active power, injected reactive power and receiving node or bus voltage (Amroune et al., 2014). The main problem is to identify the voltage instability source and one of the effective ways to achieve this, is to identify the weakest buses in the system (Oluseyi et al., 2018). This can be determined by the bus which lacks reactive power supports the most. According to Samuel et al. (2012), the 330 kV transmission lines in Nigeria national grid with a frequency of 50 Hz, which fed 23 sub-stations via 330/132 kV transformers, has a combined capacity of 6,000 MVA at a utilization factor of 80%. Similarly, the 132 kV transmission lines fed 91 sub-stations with 132/33 kV transformers of 7,800 MVA has a combined capacity at a utilization factor of 75%. This is because the grid is characterized by poor voltage profile due to overload, poor control system in most part of the grid, high transmission losses resulting to weak grid, voltage instability and eventually voltage collapse (Samuel et al., 2012; Krishnan and Nair, 2013). This motivates the examination of the power quality of the major alternative power source used in the country.

Recently, an alternative power source, photovoltaic system (PV), which is a non-linear system whose performance depends on the environmental conditions as a clean source of energy has drawn a lot of attention in recent years, considering its performance level and advantages mentioned (Akuon, 2012). A PV system can be used as a backup system and as a power consumption reduction mechanism in domestic and industrial sectors to shed essential load against commercial grid fluctuation at peak periods (Babatunde *et al.,* 2018). The application of PV systems can be categorized into two fields: standalone application and grid connected application. The PV systems used to provide power to remote loads that are not connected to the grid are referred to as the standalone applications while the grid connected PV systems are used to provide power with the utility grid (Masoud, 2013). The operation of PV systems can improve the voltage profile, reduce the energy losses of distribution feeders, cost of maintenance and loading of transformers tap changers during peak periods (Daher et al., 2008; Masoud and Hussain, 2013; Wandhare and Agarwal, 2014). PV systems can produce high voltage with high power gain coupled with less electromagnetic interference (EMI) (Rahman *et al.,* 2012).

Despite all the advantages of PV systems when compared to other renewable technologies, PV systems still have some major limitations such as harmonic pollution due to power electronics based controllers and switches, experiencing a major drawback of higher order of harmonics in the current line as a result of non-linear loads (Rahman *et al.,* 2012). This results in high cost of implementation and low efficiency due to variation in solar irradiation that can cause power fluctuation and voltage flicker. However, certain control methods have being introduced to improve the efficiency of the system such as maximum power point tracking (MPPT) (Masoud and Hussain, 2013). So also some techniques have been investigated in PV system to improve this limitation as seen in Daher et al. (2008) and Jabir et al. (2010), where a multi-transformer based PV system was introduced, to enable it to convert higher power level with the help of the high switching frequency with less ripple content. The proposed system in Rahman et al. (2012) was further improved on, in terms of reduction in high level of losses in the semiconductor coupled with less harmonics distortion in the output level in Jabir et al. (2010). This was achieved by integrating an auxiliary transformer coupled with a flying capacitor to the system.

In the available literature, power factor compensator has been recognized as the most economical and efficient way of increasing power quality (Adebayo *et al.,* 2017; Adebayo and Sun, 2018; Alayande and Nwulu 2019). This provides motivation for investigating power factor control on a standalone PV system. In this paper, the investigation is centered on the technique of reactive power compensation in a PV system connected to an inductive load, employing capacitive loads, which can generate reactive power to compensate for the lagging power factor in the system to provide voltage stabilization, good power quality and to control non-linear loads.

2. MATERIALS AND METHODS

2.1. PV System Model and Analysis

In interconnecting the PV system (PVS), some factors must be considered and satisfied. These include: phase sequence, frequency and voltage level matching (Masoud and Hussain, 2013). These factors depend on the switches and controllers of the PVS. The PVS can be expressed in terms of the current-voltage characteristics of the cell. These characteristics variation directly depends on the irradiance received by the cell and the cell temperature. Figure 1 describes a grid-connected PV system, which is the focus of this paper.

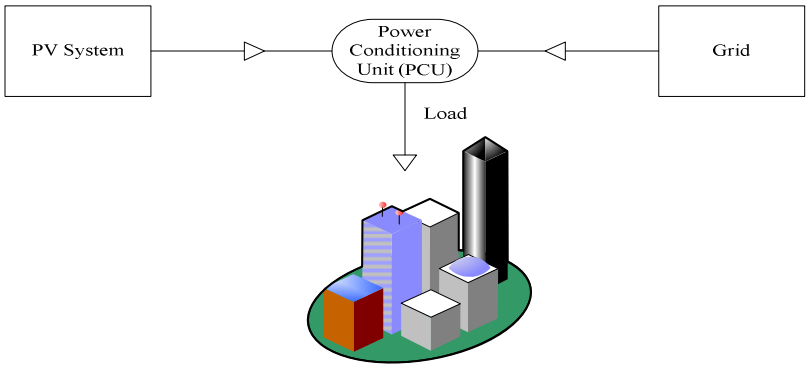

Figure 1: Grid-connected PVS

A crystalline silicon PV module is modelled in Figure 2. In order to analyze the performance of the PV systems under different weather conditions, PV arrays are interconnected in parallel-series configuration and grouped in large unit to form a PV module.

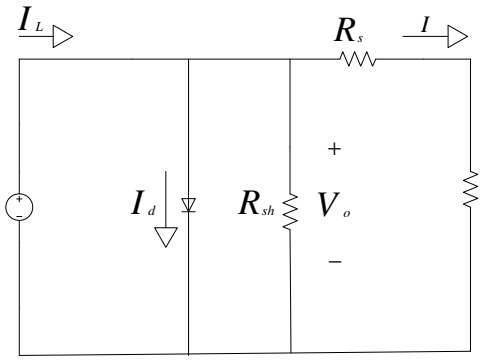

Figure 2: PV cell modelled as a diode circuit (Habyarimana and Venugopal, 2015)

Using Kirchhoff's voltage law (KVL) on Figure 2, the output current (I) can be verified as (Masoud and Hussain 2013):

$$I = I_L - I_d - \frac{V_o}{R_{sh}} \quad (1)$$

Where V_o is the shunt resistance voltage, R_{sh} is the shunt resistance, I_L is the light-generated current and I_d is the diode current which can expressed using diode current expression (Masoud and Hussain 2013) as:

$$I_d = I_o \left[e^{\frac{qV_{oc}}{nKT}} - 1 \right] \quad (2)$$

V_{oc} is the open circuit voltage which is sensitive to temperature, I_o is saturation current of the diode, q is electron ($1.6\ x\ 10^{-9}$), n is curve-fitting constant. According to Masoud and Hussain (2013), n is an ideal value between 1 and 2, K is the Boltzmann constant, which is $1.38\ x\ 10^{-9}$ J/K, T is the operating temperature given by:

$$T = T_a + \frac{T_N - 20}{800} Gc \quad (3)$$

Where Gc is the reference irradiance, T_a is the ambient air temperature, c and $T_N$is the nominal operating temperature of the cell. c is assumed in (Habyarimana and Venugopal, 2015). T_N can be expressed as:

$$T_N = T - T_a + (0.035)Gc \quad (4)$$

V_{oc} can be obtained as (Masoud and Hussain 2013):

$$V_{oc} = \left(\frac{KT}{q}\right) Ln \frac{I_L - I_o}{I_L} \quad (5)$$

Then, the output current and voltage from the solar panel are derived as function of time. The output power of the cell can be obtained in a similar way to (Masoud and Hussain 2013):

$$P = FIV \quad (6)$$

Where F is the cell fill factor and this can be formulated as (Habyarimana and Venugopal, 2015):

$$F = \frac{V_o - Ln\left(\frac{v_{oc}}{q}\right) Ln\left(\frac{qv_{oc}}{KT} + 0.72\right)}{V_o + \frac{KT}{q}} \quad (7)$$

2.2. Proposed System Topology

The regulation requires PV system to operate at a power factor equal or greater than 0.95 (Enslin 2010). The propose system measure the power factor of the PV system in real time and if the power factor is less than 0.95, then the compensation rule is adopted. Figure 3 describes the block diagram of the proposed system.

2.3. Power Factor Compensator

In the proposed system, two high frequency transformers are employed to step down the waveform. One is used to step down the current waveform while the other steps down the voltage waveform. The output of the transformers is fed to a comparator to compare two analogue voltage levels. This is then fed to the microcontroller to measure the power factor in real time. The power factor is measured using the time

difference between the current and voltage waveform, respectively by detecting the zero crossing point. If the measured power factor is less than 0.95, then the signal level at the output pin of the microcontroller will be comparatively high, thus adequately powering the relay system which connects the capacitor bank to the load, so as to initiate compensation. This is further explained by Figure 4.

For efficient analysis, the zero-crossing detector circuit is employed to quantify and assess the point at which the circuit (ac) waveform crosses the zero point in the circuit. The waveform is as depicted in Figure 5.

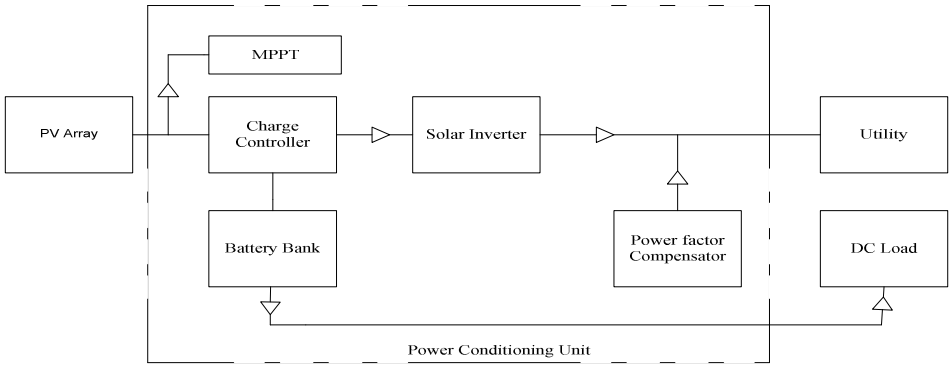

Figure 3: Block diagram of the proposed topology

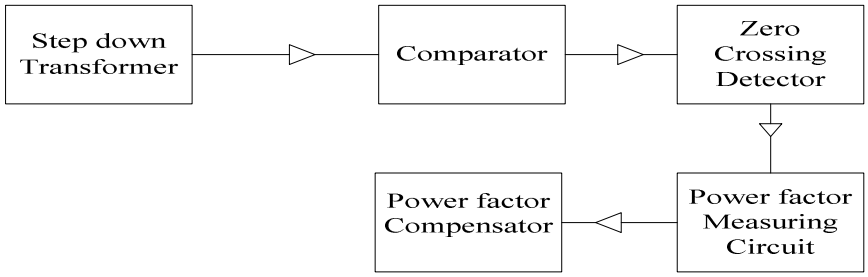

Figure 4: The proposed power factor compensator

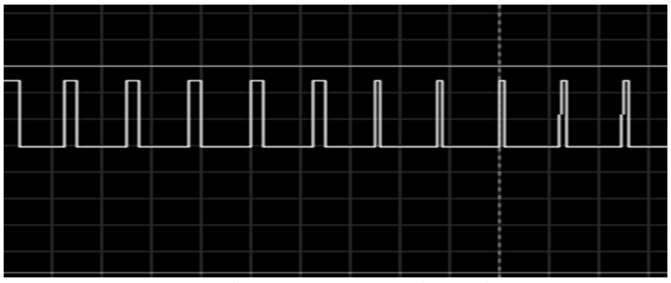

Figure 5: Zero cross detection points

Figure 5 reveals the zero crossing point of the current waveform and voltage waveform, measuring the time difference/lagging angle between the current waveform and voltage waveform. The power factor can be obtained as:

$$\theta = \text{Difference in time} \times 2\pi\text{PF} = cos(\theta) \quad (8)$$

where PF is the power factor which is multiplied by 2π to convert the time difference to radian, and θ is the time difference in radian.

2.4. Algorithm of the proposed Power Factor Compensator

Algorithm 1:

Step 1: Analyze the amplitude of the output voltage waveform of the PV system employing a transformer and comparator.

Step 2: Compute the amplitude of the output current waveform of the PV system using similar approach to step 1.

Step 3: Calculate the time difference in radian that each of the waveform. i.e. the voltage waveform and current waveform cross the zero crossing line.

Step 4: Compute the power factor employing Equation 8:

Step 5: If the computed power factor is less than 0.95 trigger on the capacitor C1 and C2 to compensate for the reactive power, else, C1 and C2 remain idle.

2.5. Analysis of the Power Factor Compensator

The required transformer can be obtained using:

$$N_1 : N_2 = \frac{V_P}{V_s} = \sqrt{\frac{L_1}{L_2}} \tag{9}$$

where N_1 and N_2 is the number of required turns of the primary side and secondary side of the transformer, respectively. Similarly, V_P and V_s is the primary and secondary voltage, respectively. L_1 and L_2 is the induction of the primary and secondary side, respectively. Likewise, the required parameters of the capacitor can be obtained using:

$$V_{dc} = V_m \left(1 - \frac{1}{2FR_LC}\right) \tag{10}$$

Where V_m is the expected peak voltage in rms, V_{dc} is the DC voltage, F is the frequency, R_L is the resistive load and C is the capacitance It can be verified from the datasheet that capacitor made from silicon have a V_m of 0.6 V. Therefore:

$$V_{dc} = V_m - 1.2 \tag{11}$$

The ripple voltage and discharge time of the capacitor can be obtained using Equations (12) and (13) respectively:

$$V_{rp} = \frac{V_{dc}}{2FR_LC} \tag{12}$$

$$T_{discharge} = \frac{1}{2F} \tag{13}$$

Where V_{rp} is the ripple voltage, R_L is the resistive load, $T_{discharge}$ is the discharge time and F is the frequency.

The power factor compensator integrated to the PV system is described in Figure 6. The microcontroller is based on C language and simulated in Porteus. The proposed system is described following the algorithm below:

Algorithm 2:

1. The output of the PV system is analyzed using a transformer and a comparator to measure the lagging angle between the voltage waveform and current waveform as they cross the zero crossing line. TR1 steps down the voltage waveform in terms of amplitude, while TR2 steps down the current waveform.

2. The output of the transformer is fed into the comparator to measure the time difference at which each waveform i.e. voltage and current waveform crossed the zero crossing line.

3. The resulting output of the comparator is fed into the microcontroller via pin 4 and 5 following the algorithm to calculate the PF.

If the PF is less than 0.95 then, pin 21 and 22 will be high to power on the relay system, which the capacitor C3 and C4 are connected to, in order to compensate for the reactive power.

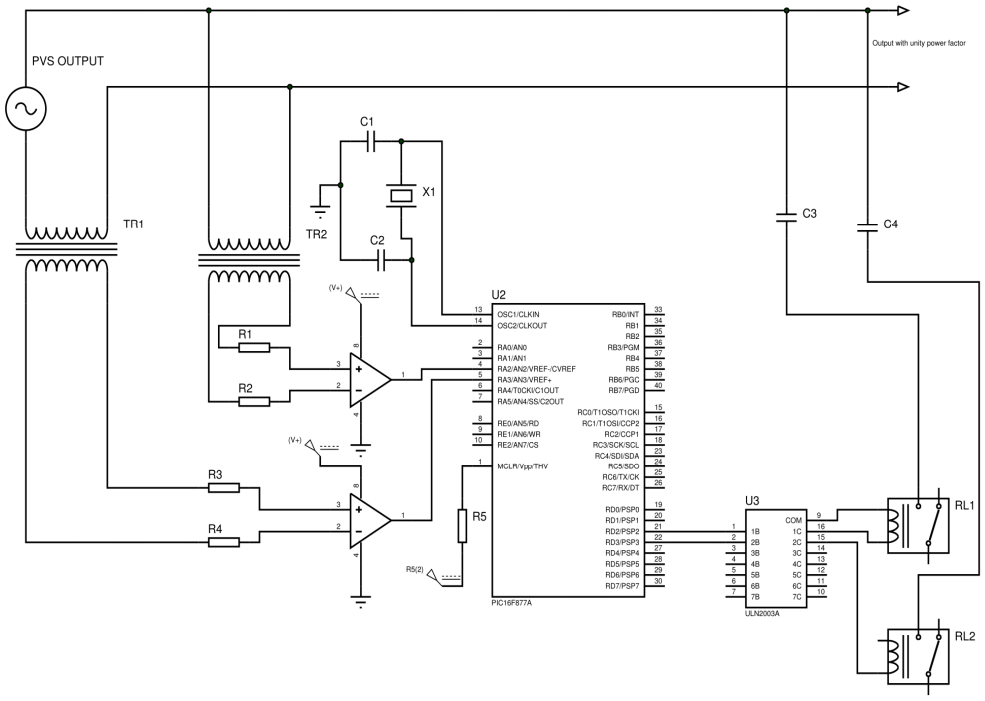

Figure 6: The Proteus model of the power factor compensator circuit

3. RESULTS AND DISCUSSION

From the obtained results, Figure 7 shows the performance characteristics of the injected reactive power at the modelled PV system connected to an inductive load. Figure 7 reveals that at first, the PV system consumed reactive power up to -1200 VA, due to the inductive load. Later, reactive power was injected to the system via the PF compensator improving the power quality up to the amount of consumed reactive power. It was observed in Figure 7 that the power factor injected at the PV system output is high. This is due to an inductive load connected to the PV system output, as inductive load is the main cause of low power factor, voltage unbalance and high reactive power (Glover *et al.,* 2012). The power factor at this point was less than unity and compensated for, as expected as seen in the waveform in Figure 8, which exhibit unstable output, considering the component of noise and ripples at the edge of the output signal.

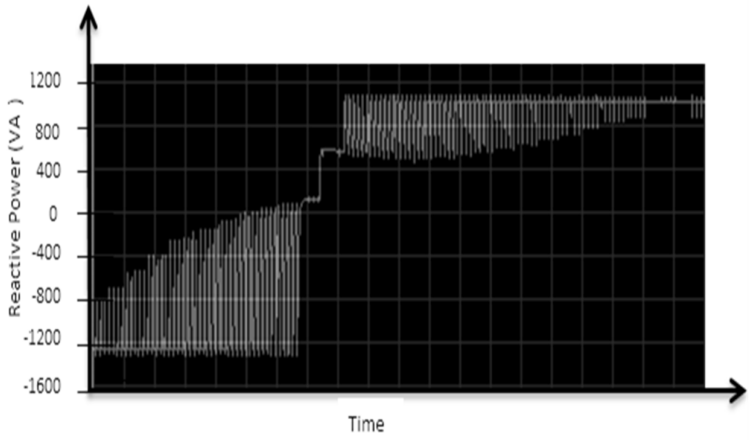

Figure 7: Injected reactive power at the PVS output

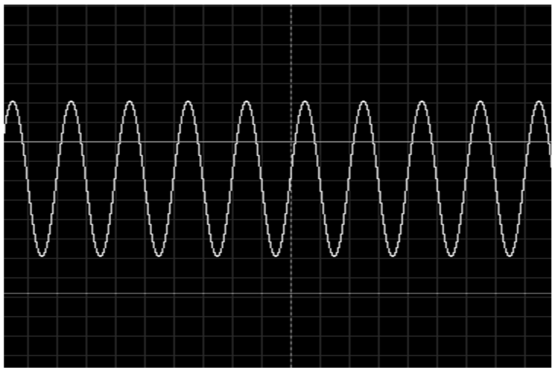

Figure 8: Output waveform of PVS with power factor less than 0.9

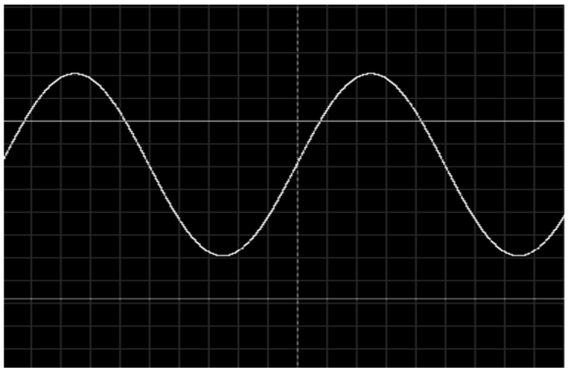

Figure 9: Output waveform of PVS with unity power factor

The power factor was compensated for employing the capacitive load integrated to the PV system, which was triggered by the microcontroller after computing the power factor in real time and the result yield a PF less than 0.95. The output waveform is presented in Figure 9, revealing a stable output waveform, which demonstrates a significant improvement when compared to Figure 8. This shows an improvement in the voltage stability of the system.

Figure 10 describes the voltage magnitude and the load current at the output of the PV system without the power factor compensator. This shows that the magnitude is a little bit unstable in relation to the load demand at that point. Thus, the power factor at this point is approximately 0.87 which is quite close to 0.95, the bench mark value. However, from this arrangement and the results obtained, the proposed system has a limitation of delay in injecting the required reactive power as seen in Figure 7. Though, the time delay is very small and this is due to the charging time delay of the capacitor but once the capacitor is charged, the required reactive power was fully compensated for as reveal in Figure 7.

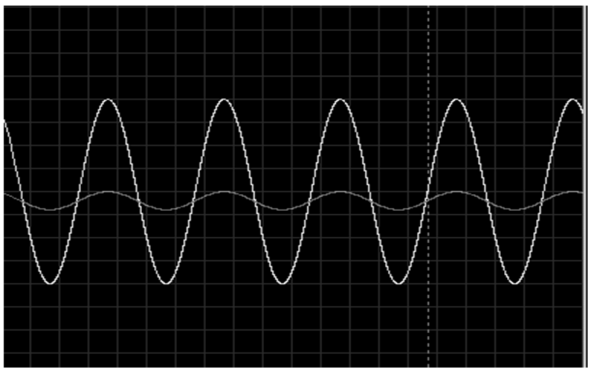

Figure 10: System voltage and current waveform

4. CONCLUSION

The power quality problems have been universally identified as one of the major setbacks of full implementation and integration of PV system's penetration in the power industry. This is mainly due to the fact that it has been identified as the major source of harmonic propagation. This work has provided a platform for the solution of the twin problems of power quality as it relates to voltage fluctuation and reversed power flow in the PV system. The technique demonstrated herein is quite an economical and efficient power factor compensation for a PV system and this can be implemented in either a grid-connected or standalone PV system.

5. CONFLICT OF INTEREST

There is no conflict of interest associated with this work.

REFERENCES

Adebayo, I., Jimoh, A. A. and Yusuff, A. (2017). Voltage stability assessment and identification of important nodes in power transmission network through network response structural characteristics. *IET Generation, Transmission & Distribution,* 11(6), 1398-1408.

Adebayo, I. G. and Sun, Y. (2018). Voltage Stability Enhancement Capabilities of LTCT and STATCOM in a Power System. In 2018 *IEEE PES/IAS PowerAfrica*, pp. 1-560.

Akuon, P. O. (2012). Optimized hybrid green power model for remote telecom sites. In *IEEE Power and Energy Society Conference and Exposition in Africa: Intelligent Grid Integration of Renewable Energy Resources (PowerAfrica)* (pp. 1-5).

Alayande, A. S. and Nwulu, N. (2019). A novel approach for the identification of critical nodes and transmission lines for mitigating voltage instability in power networks. *African Journal of Science, Technology, Innovation and Development,* 11(3), pp. 383-390.

Amroune, M., Bourzami, A. and Bouktir, T. (2014). Weakest buses identification and ranking in large power transmission network by optimal location of reactive power supports. *TELKOMNIKA Indonesian Journal of Electrical Engineering*, *12*(10), pp. 712-730.

Babatunde, D. E., Babatunde, O. M., Akinbulire, T. O. and Oluseyi, P. O. (2018). Hybrid energy systems model with the inclusion of energy efficiency measures: A rural application perspective. *International Journal of Energy Economics and Policy*, 8(4), pp. 310-323.

Bayliss, C. R., Bayliss, C. and Hardy, B. (2012). *Transmission and distribution electrical engineering*. Elsevier.

Daher, S., Schmid, J. and Antunes, F. L. (2008). Multilevel inverter topologies for stand-alone PV systems. *IEEE transactions on industrial electronics*, *55*(7), pp. 2703-2712.

Enslin, J. H. (2010). Network impacts of high penetration of photovoltaic solar power systems. In *IEEE PES General Meeting*, pp. 1-5.

Farhoodnea, M., Mohamed, A., Shareef, H. and Zayandehroodi, H. (2013). Power quality analysis of grid-connected photovoltaic systems in distribution networks. *Przeglad Elektrotechniczny (Electrical Review)*, *2013*, pp. 208-213.

Glover, J. D., Sarma, M. S. and Overbye, T. (2012). *Power system analysis & design, SI version*. Cengage Learning.

Gonen, T. (2015). *Electric power distribution engineering*. CRC press.

Habyarimana, M. and Venugopal, C. (2015). Automated hybrid solar and mains system for peak time power demand. In: *2015 International Conference on the Domestic Use of Energy (DUE,)* pp. 169-175.

Jabir, H., Mekhilef, S., Nakaoka, M. and Nishida, K. (2013). Development of a transformer-based multilevel inverter topology for stand-alone photovoltaic system. In: *2013 15th European Conference on Power Electronics and Applications (EPE),* pp. 1-10.

Kang, F. S., Rhee, K. Y., Park, S. J., Moon, C. J. and Ise, T. (2004). New approach for cascaded-transformers-based multilevel inverter with an efficient switching function. In *30th Annual Conference of IEEE Industrial Electronics Society, 2004. IECON 2004*, Vol. 2, pp. 1805-1810.

Krishnan, K. M. and Nair, P. C. (2013). Measurement and analyses of power quality problems associated with a grid having wind energy conversion systems. In *2013 International Conference on Energy Efficient Technologies for Sustainability*, pp. 590-595.

Madhusudan, R. and Rao, G. R. (2012). Modeling and simulation of a distribution STATCOM (D-STATCOM) for power quality problems-voltage sag and swell based on Sinusoidal Pulse Width Modulation (SPWM). In *IEEE-International Conference on Advances in Engineering, Science and Management (ICAESM-2012)*, pp. 436-441.

Masoud, F.A.M. and Hussain, S. (2013). Power Quality Analysis of Grid-Connected Photovoltaic Systems in Distribution Networks. *PRZEGLĄD ELEKTROTECHNICZNY*, pp. 208-213.

Oluseyi, P.O., Ajekigbe, T.O., Babatunde, O.M. and Akinbulire, T.O. (2018). Assessment of electrical grid fragility in Nigeria-31 bus system. *Arid Zone Journal of Engineering, Technology and Environment*, 14(4), pp. 713-726.

Rahman, K., Tariq, A. and Bakhsh, F. I. (2012). Modeling and analysis of multilevel inverters using unipolar and bipolar switching schemes. In: *IEEE-International Conference on Advances in Engineering, Science and Management (ICAESM-2012)*, pp. 466-471.

Rohouma, W., Balog, R. S., Peerzada, A. A. and Begovic, M. M. (2019, May). Reactive Power Compensation of Time-Varying Load Using Capacitor-less D-STATCOM. In: *2019 10th International Conference on Power Electronics and ECCE Asia (ICPE 2019-ECCE Asia)*, pp. 2296-230.

Samuel, I., Katende, J. and Ibikunle, F. (2012). Voltage Collapse and the Nigerian National Grid. In *EIE's 2nd International Conference on Computer Energy Networks Robotics and Telecommunication*, pp. 128-131.

Wandhare, R. G. and Agarwal, V. (2014). Reactive power capacity enhancement of a PV-grid system to increase PV penetration level in smart grid scenario. *IEEE Transactions on Smart Grid*, *5*(4), pp. 1845-1854.